SUPPORTING INFORMATION

Black mesoporous anatase TiO_2 nanoleaves: A high capacity and high rate anode for aqueous Al-ion batteries

Ying Juan He, [a] Jun Fang Peng, [a] Wei Chu, *[b] Yuan Zhi Li [a] and Dong Ge Tong*[a]

[a]Mineral Resources Chemistry Key Laboratory of Sichuan Higher Education Institutions, College of Materials and Chemistry & Chemical Engineering, Chengdu University of Technology, Chengdu 610059, China. E-mail: tongdongge@163.com; Fax: +86-28-8407 9074

[b]College of Chemical Engineering, Sichuan University, Chengdu 610065, China. E-mail: chuwei65@foxmail.com; Fax: +86-28-8540 3397

Summary: 20 Pages; 2 Tables; 26 Figures;

Table S1 XRD Rietveld refinement results and conductivity of the samples

Samples	Composition	a / nm	c / nm	Rp/%	Rwp/%	Rb/%	Conductivity/ Scm^{-1}
commercial white anatase TiO_2	TiO_2	0.38007(3)	0.94898(4)	8.09	6.01	4.12	9.7×10^{-7}
black anatase TiO_2 nanoleaves	$TiO_{1.976}(NH)_{0.024}$	0.38124(2)	0.95099(1)	8.23	5.45	4.04	3.0×10^{-1}
commercial white anatase TiO_2 after SPP treatment with NH_4Cl	$TiO_{1.983}(NH)_{0.017}$	0.38092(4)	0.95075(7)	8.75	5.89	4.07	9.9×10^{-2}
white anatase TiO_2[18]	TiO_2	0.3887(7)	0.94894(7)	-	-	-	2.2×10^{-7}
black anatase TiO_2[18]	$TiO_{1.974}(NH)_{0.026}$	0.38038(3)	0.95148(7)	-	-	-	8.2×10^{-2}

Table S2 Impedance parameters of the samples

Samples	Cycles	R_e / Ω	R_{sei} / Ω	R_{ct} / Ω	Z_w / Ω
Commercial white TiO_2 anatase	no cycling	1.2	-	68.7	203
	the 1st cycle	1.8	2.3	103.1	70.6
	the 10th cycle	2.6	2.7	72.0	47.5
	the 30th cycle	3.9	3.2	79.2	55.5
	the 50th cycle	4.2	3.6	85.3	60.3
Black anatase TiO_2 nanoleaves	no cycling	1.1	-	24.7	65.2
	the 1st cycle	1.7	4.8	30.8	20.4
	the 10th cycle	2.4	5.2	16.7	18.7
	the 30th cycle	3.7	5.4	17.8	19.6
	the 50th cycle	4.2	5.6	18.5	20.3

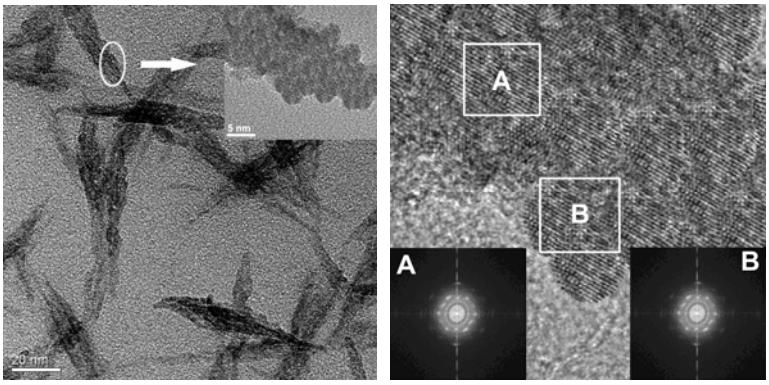

(a) (b)

Fig.S1 (a) High magnification TEM image (the inset is the enlargement of the frame), and (b) the FFT patterns originated from the marked areas in the HRTEM image of the as-prepared black anatase TiO_2 nanoleaves.

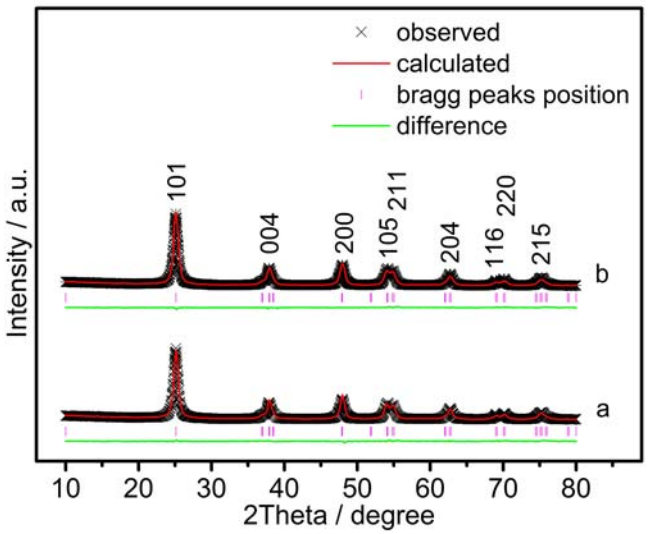

Fig.S2 XRD Rietveld refinement for the diffraction patterns of (a) the commercial white anatase TiO_2 and (b) the commercial white anatase TiO_2 after treated by SPP with NH_4Cl.

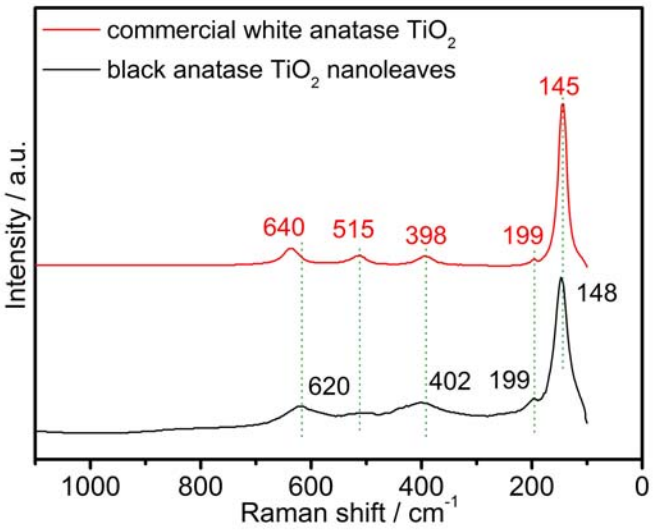

Fig.S3 Raman spectra of the commercial white anatase TiO_2 and black anatase TiO_2 nanoleaves.

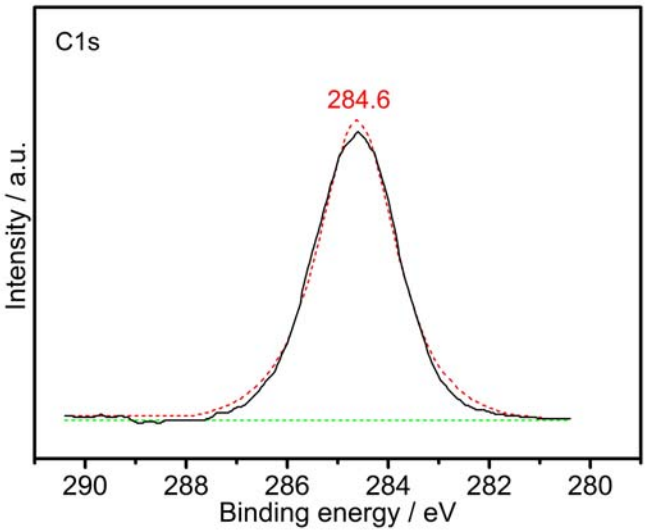

Fig.S4 C1s high-resolution XPS spectrum for the black anatase TiO_2 nanoleaves.

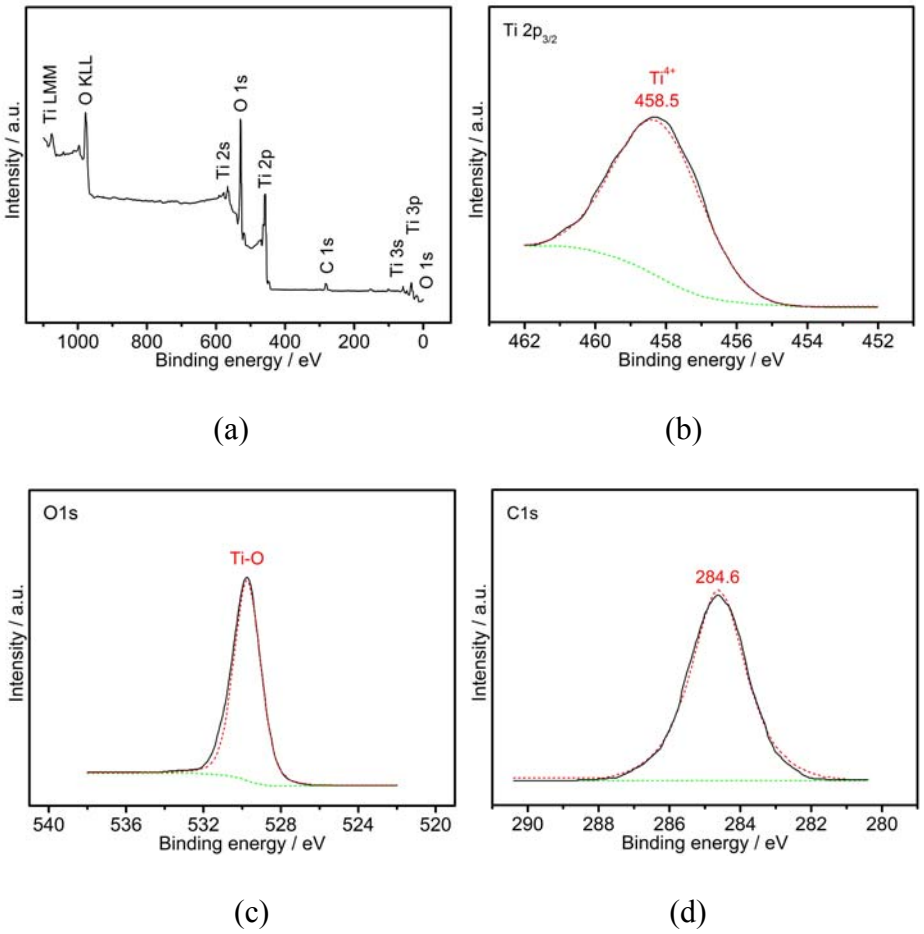

Fig.S5 XPS spectra for the commercial white anatase TiO_2: (a) survey spectrum; (b) Ti $2p_{3/2}$; (c) O 1s and (d) C 1s high-resolution spectra.

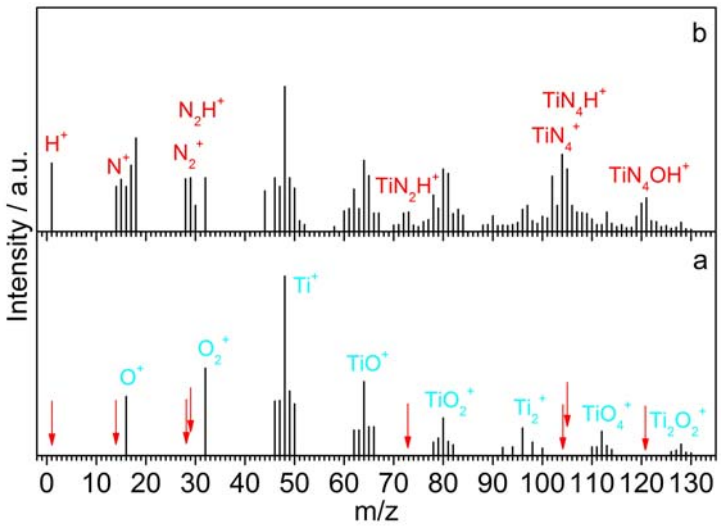

Fig.S6 ToF-SIMS spectra of (a) the commercial white anatase TiO_2 and (b) the commercial white anatase TiO_2 after treated by SPP with NH_4Cl.

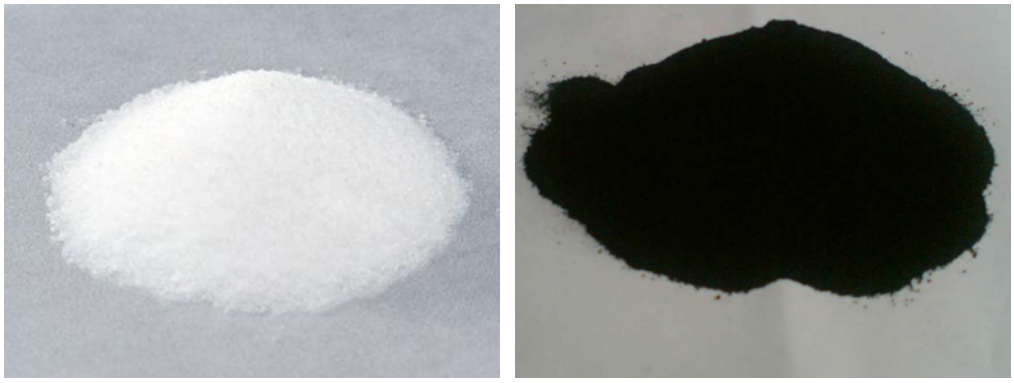

(a) **(b)**

Fig.S7 Photographs of (a) the commercial white anatase TiO_2 nanoleaves and (b) the commercial white anatase TiO_2 nanoleaves after treated by SPP with NH_4Cl.

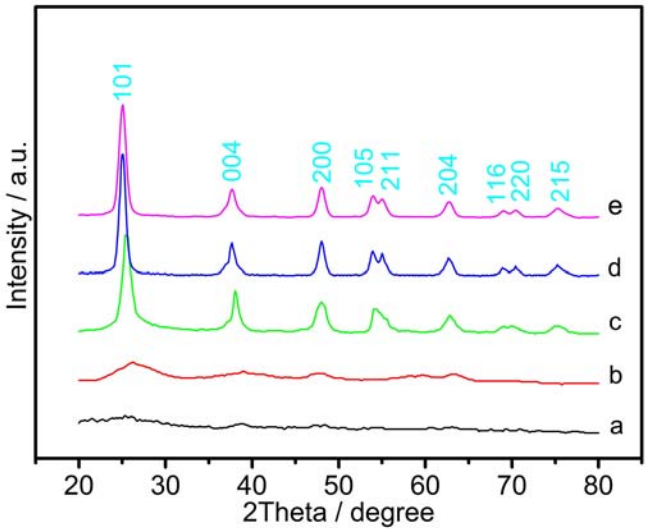

Fig.S8. XRD patterns of the black anatase TiO_2 nanoleaves prepared during SPP: (a) 0.5 min; (b) 1 min; (c) 2 min; (d) 5 min; (e) 10 min.

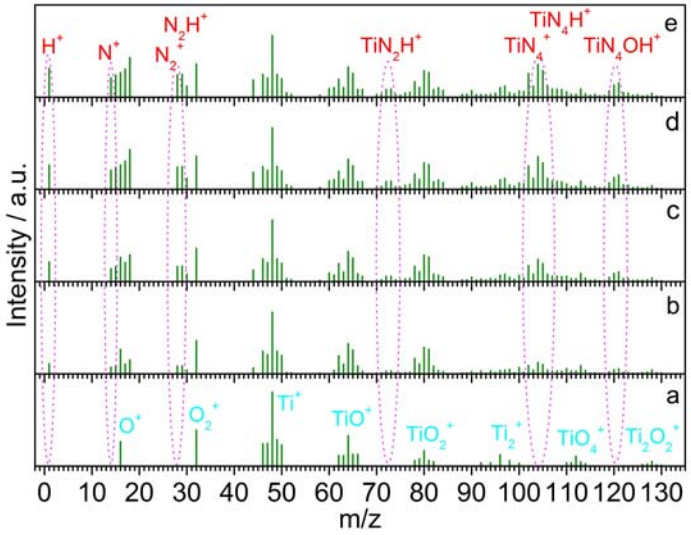

Fig.S9. ToF-SIMS spectra of the black anatase TiO_2 nanoleaves prepared during SPP: (a) 0.5 min; (b) 1 min; (c) 2 min; (d) 5 min; (e) 10 min.

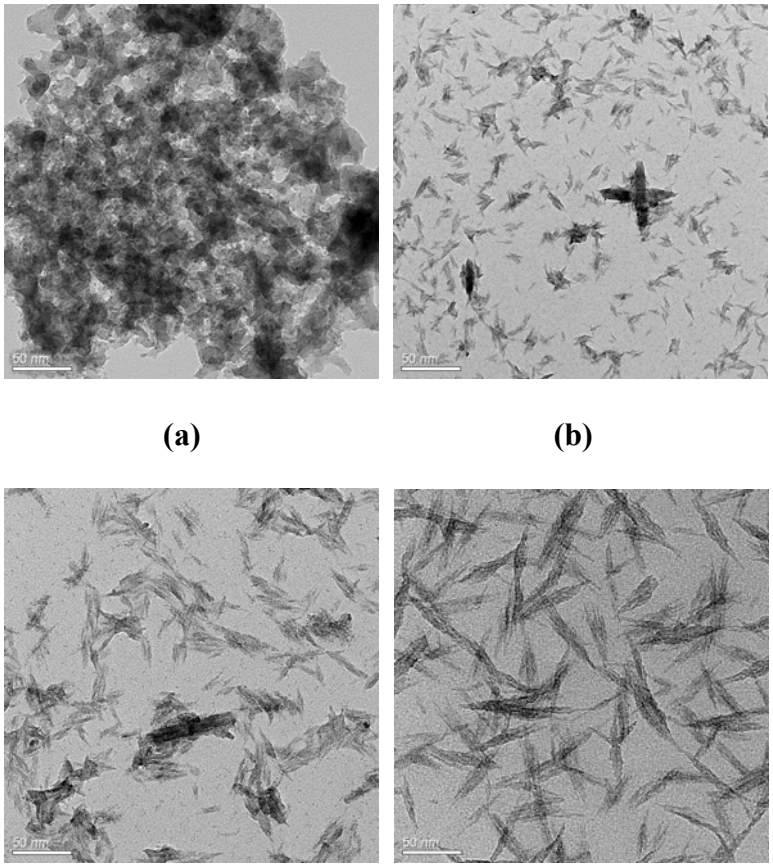

(a) **(b)**

(c) **(d)**

Fig.S10 TEM images of the black anatase TiO_2 nanoleaves obtained with different concentration of Brij-30: (a) 0 M, (b) 0.01 M, (c) 0.02M, (d) 0.05 M.

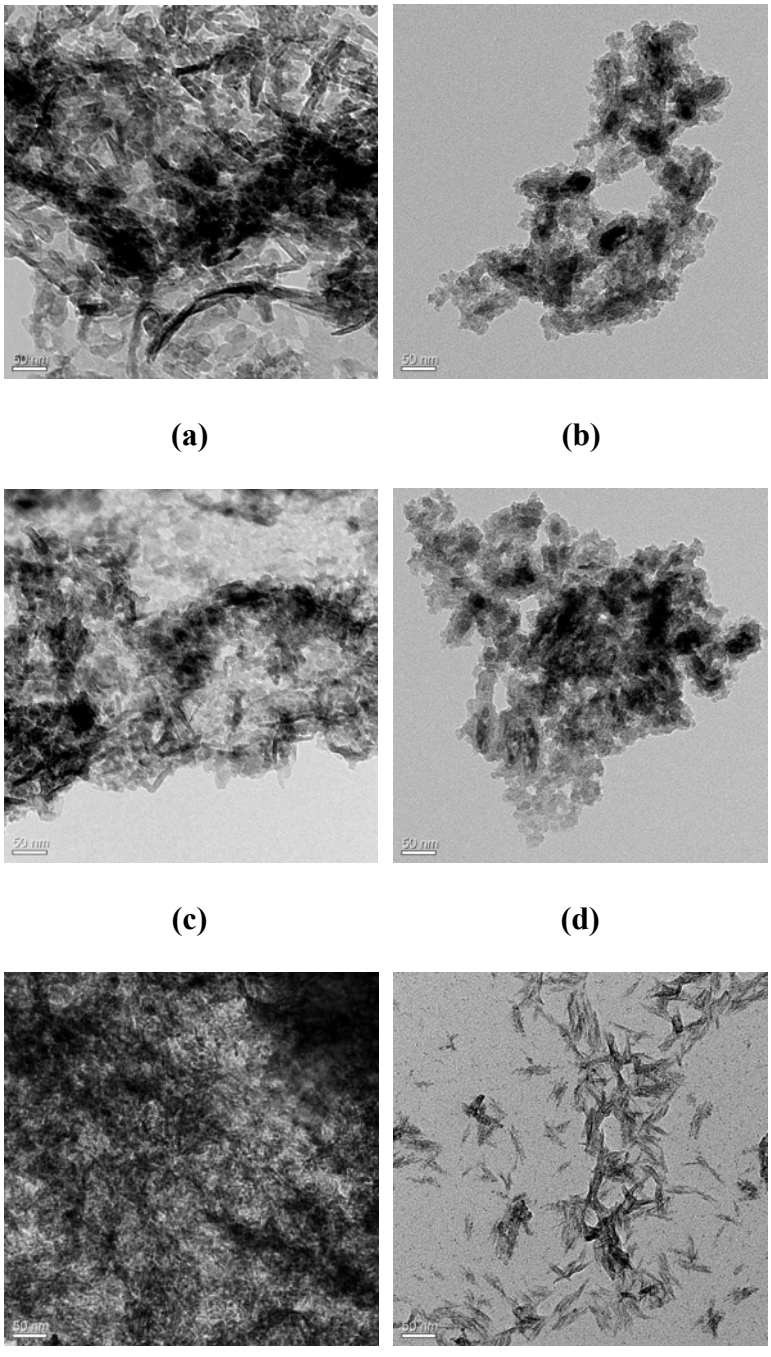

Fig.S11. TEM images of the black anatase TiO_2 nanoleaves prepared by SPP with (a) P123; (b) ethylenediamine; (c) SDBS; (d) PVA; (e) PVP and (f) either of (a)–(e) after additional of Brij-30.

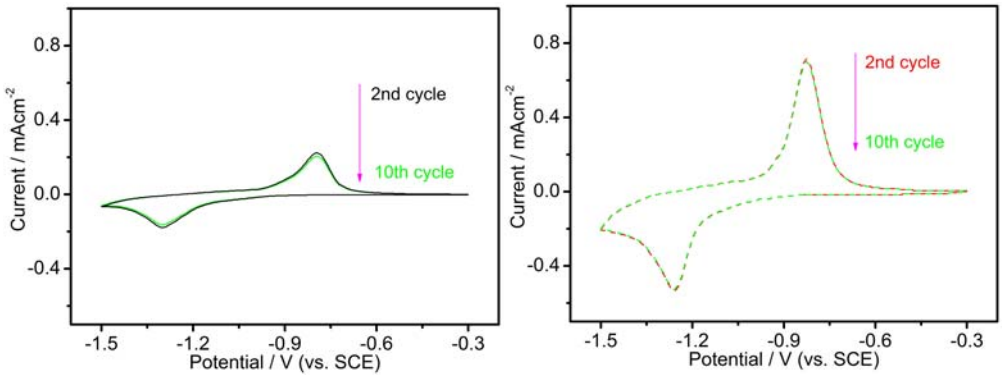

(a) **(b)**

Fig.S12 Cyclic voltammograms of (a) commercial white anatase TiO_2 and (b) black anatase TiO_2 nanoleaves electrodes at a scanning rate of $1mVs^{-1}$ from the second to the tenth cycle.

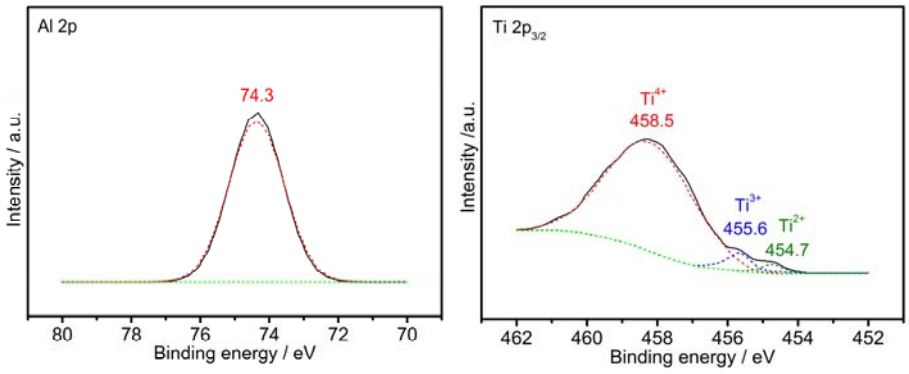

(a) **(b)**

Fig.S13 XPS spectra of the commercial white anatase TiO_2 after being 1st discharged at 0.05 Ag^{-1} between -1.4 and - 0.4 V (vs. SCE) with argon-ion sputtering for 3 min: (a) Al 2p and (b) Ti $2p_{3/2}$.

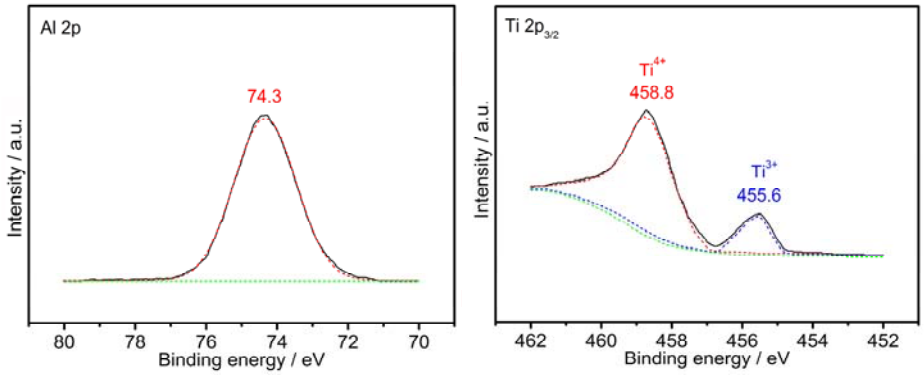

(a) **(b)**

Fig.S14 XPS spectra of the black anatase TiO_2 nanoleaves after being 1st discharged at 0.05 Ag^{-1} between -1.4 and - 0.4 V (vs. SCE) with argon-ion sputtering for 3 min: (a) Al 2p and (b) Ti $2p_{3/2}$.

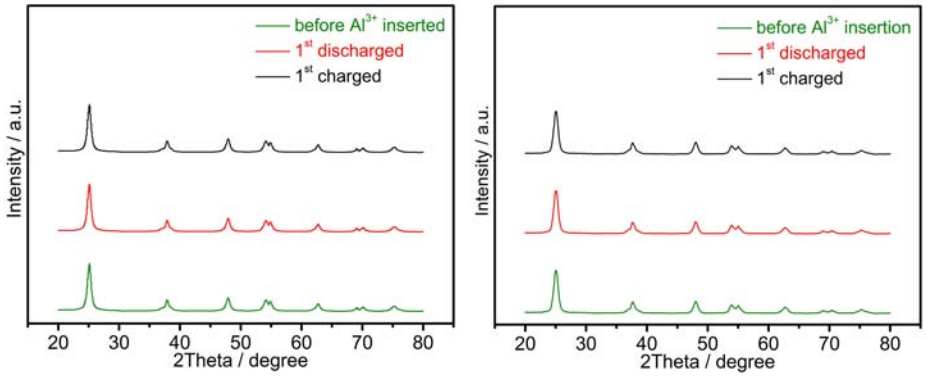

(a) **(b)**

Fig.S15 XRD patterns of the (a) commercial white anatase TiO_2; (b) black anatase TiO_2 nanoleaves before Al^{3+} insertion and after being 1st discharged and charged at 0.05 Ag^{-1} between -1.4 and - 0.4 V (vs. SCE).

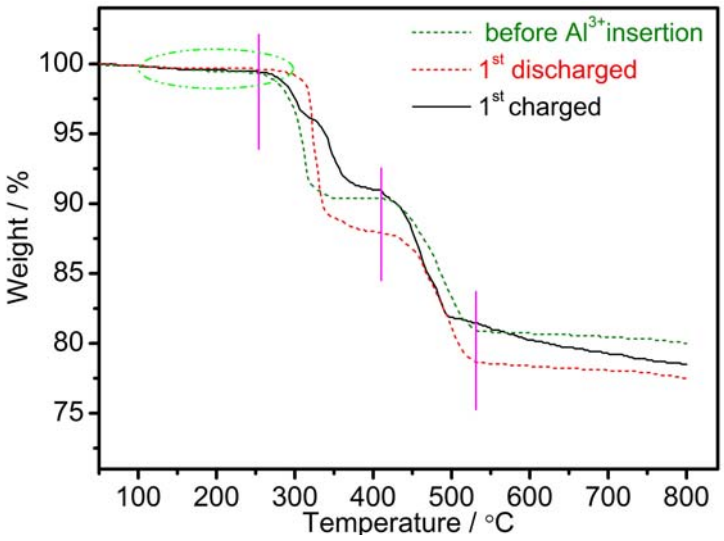

Fig.S16 The typical curves of black anatase TiO_2 nanoleaves before Al^{3+} insertion and after being 1st discharged and charged at 0.05 Ag^{-1} between -1.4 and - 0.4 V (vs. SCE).

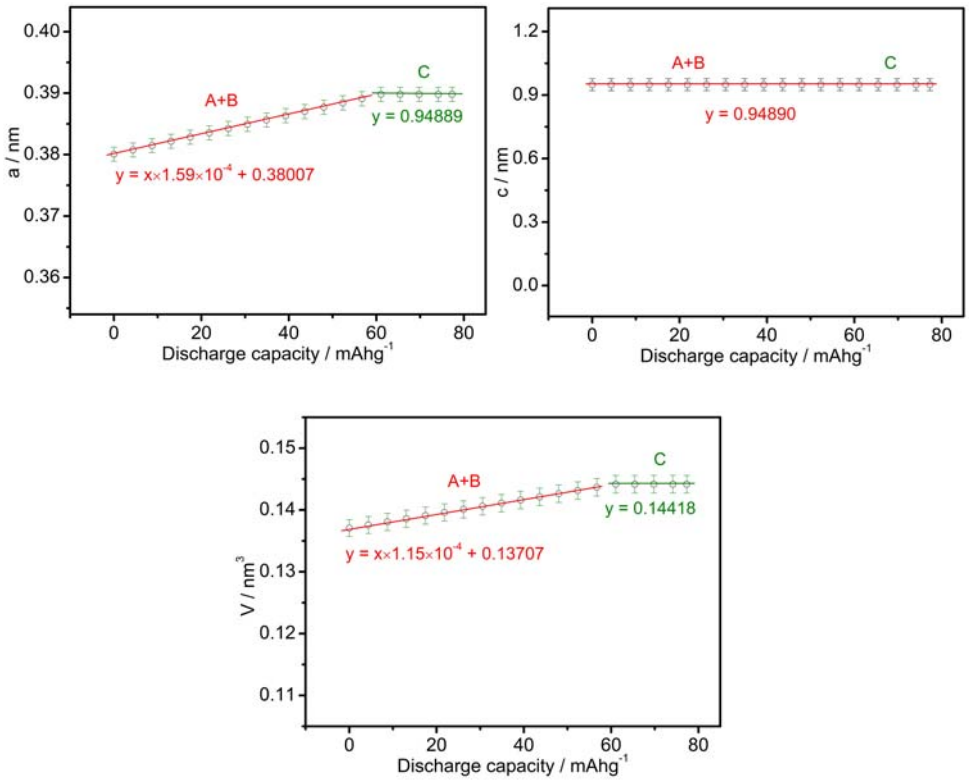

Fig.S17 The changes of crystal parameters (*a, c* and lattice volume *V*) of commercial white anatase TiO_2 obtained from the in-situ XRD in A, B and C regions labeled in Fig.8 during the 1st discharge at 0.05 Ag^{-1} between -1.4 and - 0.4 V (vs. SCE).

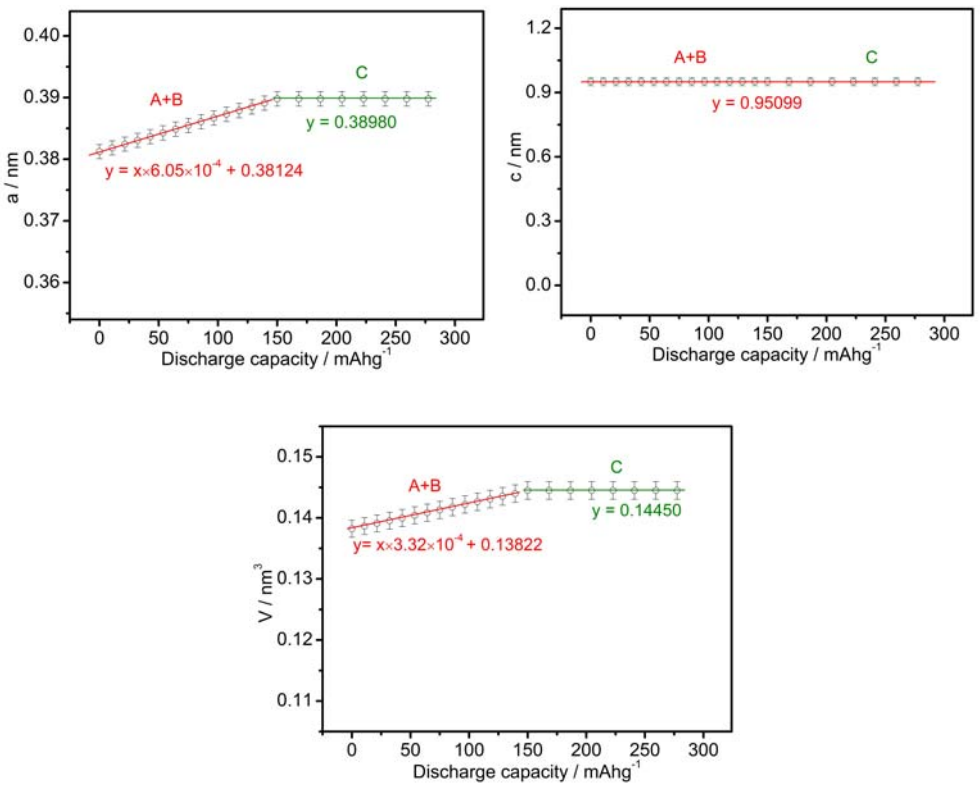

Fig.S18 The changes of crystal parameters (a, c and lattice volume V) of black anatase TiO_2 nanoleaves obtained from the in-situ XRD in A, B and C regions labeled in Fig.8 during the 1st discharge at 0.05 Ag^{-1} between -1.4 and - 0.4 V (vs. SCE).

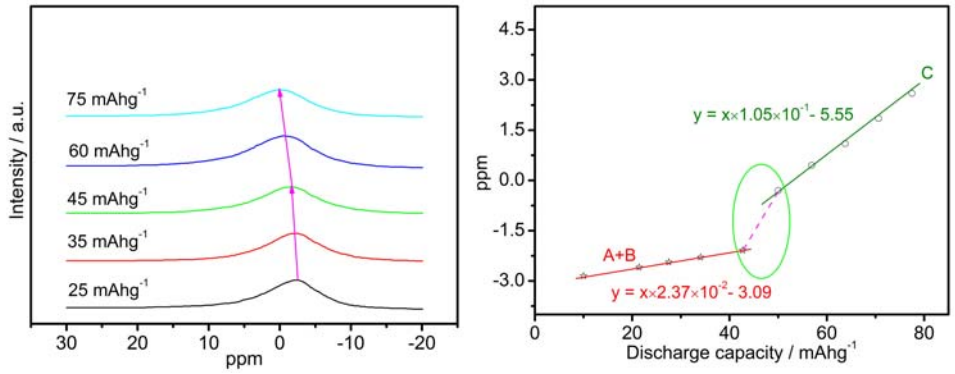

(a) **(b)**

Fig.S19 (a) The typical *ex situ* ^{27}Al MAS NMR curves and (b) the variation of shifts of commercial white anatase TiO_2 in A, B and C regions labeled in Fig.8 during the 1st discharge at 0.05 Ag^{-1} between -1.4 and - 0.4 V (vs. SCE).

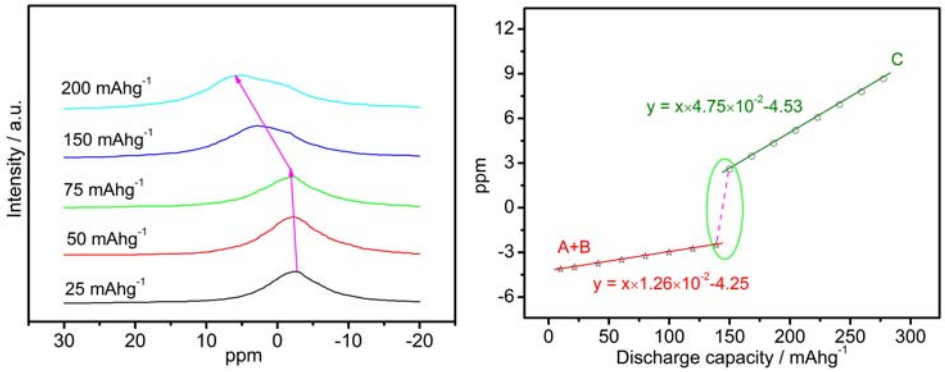

(a) **(b)**

Fig.S20 (a) The typical in-situ ^{27}Al MAS NMR curves and (b) the variation of shifts of black anatase TiO_2 nanoleaves in A, B and C regions labeled in Fig.8 during the 1st discharge at 0.05 Ag^{-1} between -1.4 and - 0.4 V (vs. SCE).

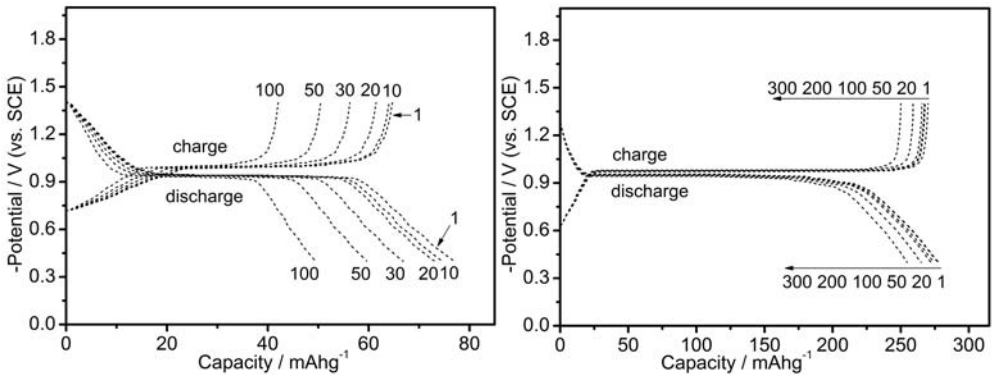

(a) **(b)**

Fig.S21 Charge-discharge curves of (a) commercial white anatase TiO_2 and (b) black anatase TiO_2 nanoleaves electrodes under a current rate of 0.05 Ag^{-1} at different cycles.

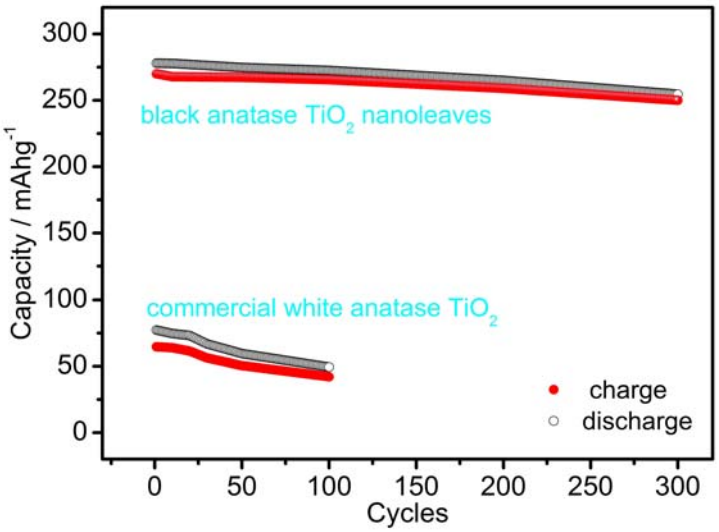

Fig.S22 Cycle performance of commercial white anatase TiO_2 and black anatase TiO_2 nanoleaves electrodes at a current rate of 0.05 Ag^{-1}.

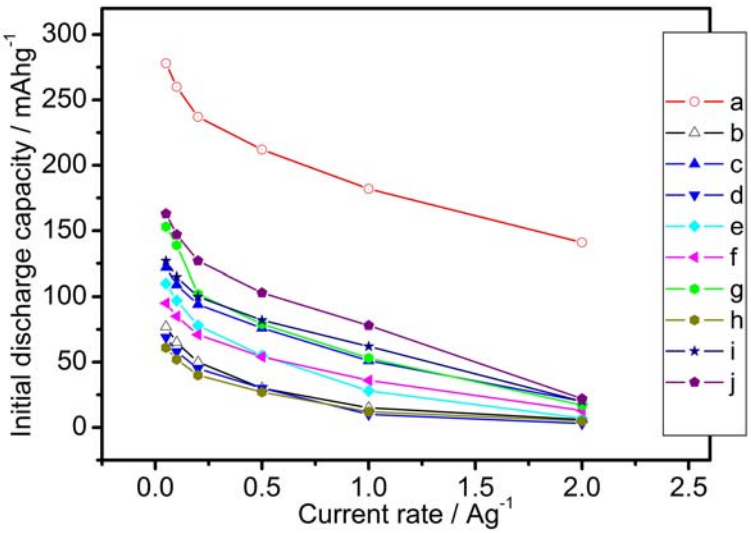

Fig.S23 Rate performance comparison of the samples (a) black anatase TiO_2 nanoleaves in this work; (b) commercial white anatase TiO_2; (c) black anatase TiO_2 prepared from (b) after SPP treatment with NH_4Cl; (d) commercial TiO_2-P25; (e) commercial anatase TiO_2-UV100; (f) commercial white anatase TiO_2 nanotube; (g) black anatase TiO_2 nanotubes prepared from (f) after SPP treatment with NH_4Cl; (h) amorphous white anatase TiO_2 obtained in our work after SPP for 0.5 min; (i) black anatase TiO_2 obtained in our work after SPP for 1 min; (j) black anatase TiO_2 obtained in our work after SPP for 2 min.

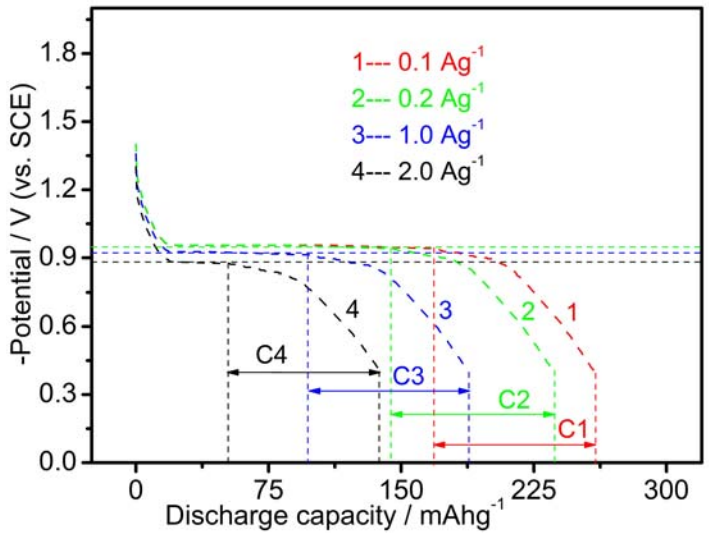

Fig.S24 The 1st insertion curves at various rates of the TiO_2 nanoleaves.

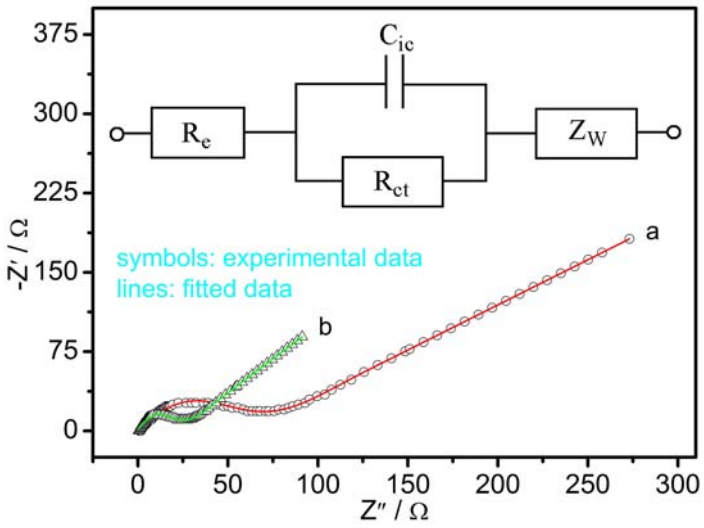

Fig.S25 Nyquist plots with fitted lines of (a) commercial white anatase TiO_2 and (b) black anatase TiO_2 nanoleaves. The inset is the corresponding equivalent circuits.

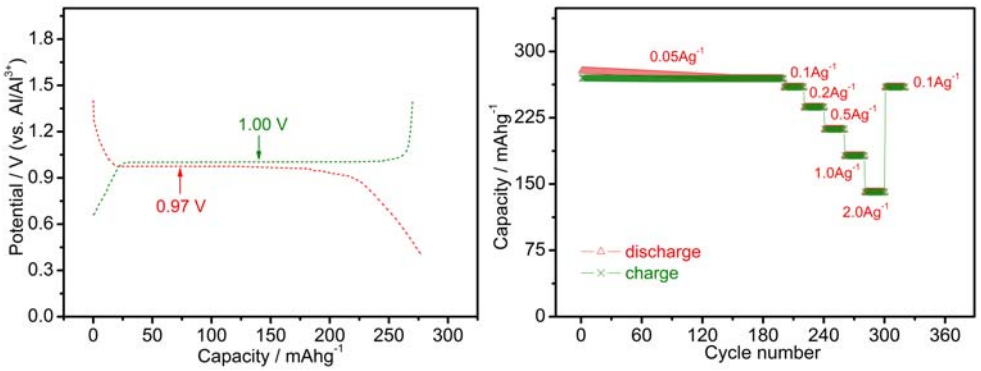

(a) **(b)**

Fig.S26 (a) The initial charge/discharge curves and (b) the variation of charge/discharge capacities with cycle numbers of TiO_2/Al two-electrode cell at different current rates between 0.4 and 1.4 V (vs. Al/Al^{3+})